



# Exogenous Spermidine Alleviates Diabetic Myocardial Fibrosis Via Suppressing Inflammation and Pyroptosis in db/db Mice

Can Wei<sup>#1,2</sup>, Jiyu Xu<sup>#3</sup>, Yong Liu<sup>4</sup>, Javeria Qadir<sup>5</sup>, Shumin Zhang<sup>6</sup>, Hui Yuan<sup>1,6</sup>

<sup>1</sup>School of Basic Medical Sciences, Mudanjiang Medical University, Mudanjiang, China

<sup>2</sup>Department of Pathophysiology, Harbin Medical University, Harbin, China

<sup>3</sup>School of Medical Imaging, Mudanjiang Medical University, Mudanjiang, China

<sup>4</sup>Animal Research Institute, Research Department, Mudanjiang Medical University, Mudanjiang, China

<sup>5</sup>Department of Biosciences, COMSATS University Islamabad, Islamabad, Pakistan

<sup>6</sup>School of Stomatology, Mudanjiang Medical University, Mudanjiang, China

<sup>#</sup>These authors contributed equally.

**Background:** The main pathological feature of diabetic cardiomyopathy (DCM) caused by diabetes mellitus is myocardial fibrosis. According to recent studies in cardiology, it has been suggested that spermidine (SPD) has cardioprotective properties.

**Aims:** To explore the role and mechanism of SPD in alleviating myocardial fibrosis of DCM.

**Study Design:** In vivo and in vitro study.

**Methods:** Type 2 diabetic mice and primary neonatal mouse cardiac fibroblasts (CFs) were selected. Measurements of serum-related markers, echocardiographic analysis, and immunohistochemistry were used to evaluate myocardial fibrosis injury and the effects of SPD. The proliferation and migration of CFs undergoing different treatments were studied. Immunoblotting and real-time quantitative reverse transcription polymerase chain reaction were used to demonstrate molecular mechanisms.

**Results:** In vivo immunoblotting analysis indicated a downregulation of ornithine decarboxylase and an upregulation of SPD/spermine

N1-acetyltransferase. We observed cardiac dysfunction in diabetic mice after 12 weeks. However, the administration of exogenous SPD improved cardiac function, decreased collagen deposition, and reduced myocardial tissue damage. mRNA expression levels of NLRP3, Caspase-1, GSDMD-N, interleukin (IL)-1 $\beta$ , IL-17A, and IL-18 were increased and suppressed in the myocardium of db/db mice upon treatment with SPD. SPD inhibited the proliferation, migration, and collagen secretion of high-glucose-treated fibroblasts in vitro. SPD inhibits the activation of the TGF- $\beta$ 1/Smad signaling pathway and decreases collagen deposition by reducing pyroptosis and Smad-7 ubiquitination levels.

**Conclusion:** Based on our findings, SPD may have potential applications in protecting against the deterioration of cardiac function in patients with DCM due to a significant new mechanism for diabetic myocardial fibrosis that we discovered.

## INTRODUCTION

Diabetic cardiomyopathy (DCM), one of the most severe complications of diabetes mellitus,<sup>1</sup> differs from myocardial lesions caused by hypertension, coronary disease, valvular disease, and other heart diseases. DCM-affected myocardial tissue reveals significant metabolic abnormalities and distinct microvascular

lesions that can progress to diffuse necrosis, leading to various abnormal cardiac functions. Myocardial fibrosis is one of the common pathological manifestations.<sup>2</sup> It is a pathological process characterized by an unsteady imbalance of the extracellular matrix, in which the proportion of various types of collagen fibers appears to be maladjusted, as well as changes in the structure of myocardial tissue and the number of inflammatory mediators, all of which affect



Corresponding author: Hui Yuan, School of Basic Medical Sciences, Mudanjiang Medical University, Mudanjiang, China  
e-mail: huiyuan1982@126.com

Received: March 01, 2023 Accepted: June 01, 2023 Available Online Date: September 07, 2023 • DOI: 10.4274/balkanmedj.galenos.2023.2023-3-102

Available at [www.balkanmedicaljournal.org](http://www.balkanmedicaljournal.org)

ORCID iDs of the authors: C.W. 0000-0003-4291-7653; J.X. 0009-0006-7731-5723; Y.L. 0000-0002-6999-4272; J.Q. 0000-0001-7200-3778; S.Z. 0009-0001-6419-812X; H.Y. 0000-0001-5646-9447.

Cite this article as:

Wei C, Xu J, Liu Y, Qadir J, Zhang S, Yuan H. Exogenous Spermidine Alleviates Diabetic Myocardial Fibrosis Via Suppressing Inflammation and Pyroptosis in db/db Mice. *Balkan Med J*; 2023; 40(5):333-43.

Copyright@Author(s) - Available online at <http://balkanmedicaljournal.org/>

the physiological functioning of the heart.<sup>3</sup> Unfortunately, the exact pathogenesis of DCM myocardial fibrosis remains unknown.

Spermidine (SPD), small positively charged molecules with branched chains derived from linear amino acids, is one of the most common polyamines found in all types of mammalian cells.<sup>4</sup> The metabolism of SPD in organisms is regulated by two enzymes: ornithine decarboxylase (ODC) and SPD/spermine-N1-acetyltransferase (SSAT). The former is the anabolic rate-limiting enzyme, and the latter is the catabolic rate-limiting enzyme. Synergistic effects between the two enzymes control the level of SPD in the biological organism.<sup>5,6</sup> SPD has many functions in an organism, including DNA synthesis, gene transcription, protein translation, cell cycle progression, cell senescence, and apoptosis.<sup>7</sup> Several studies have focused on the impact of SPD on the aging process, demonstrating its ability to enhance mitochondrial biogenesis and function.<sup>4,8,9</sup> Newer studies indicate that SPD can alleviate cardiac injury by reducing stress damage;<sup>5</sup> however, no research has been conducted to date to investigate the effects of SPD on diabetic myocardial fibrosis.

Recent studies have confirmed that diabetic rats exhibit decreased levels of SPD and spermine<sup>10,11</sup> and that administering exogenous spermine can protect cardiomyocytes from hyperglycemia and hyperlipidemia damage in rats.<sup>12,13</sup> As an intermediary in the spermine synthesis process, SPD may have beneficial effects on diabetic myocardial fibrosis, but this still needs to be validated. In the present study, we evaluated the therapeutic implications of SPD in the development of myocardial fibrosis using a type 2 diabetic mouse model, and we determined the underlying therapeutic molecular mechanisms of SPD by examining cardiac fibroblasts (CFs) exposed to high-glucose levels.

## MATERIALS AND METHODS

### Experimental animals

Eight-week-old mice ( $20 \pm 0.5$  g) were provided by the Animal Research Institute of Mudanjiang. The study was approved by the Mudanjiang Medical University (MMU) Medical Science Ethics Committee all animals were bred in an SPF-level laboratory and divided into three groups ( $n = 8$  per group): (a) wild-type (WT) group consisting of C57BL/6 mice that received 0.9% sodium chloride injections, (b) T2D group consisting of db/db mice, (c) T2D + SPD group consisted of db/db mice that received intraperitoneal injections of SPD (10 mg/kg in 0.9% sodium chloride) every other day. All mice were sacrificed at the end of week 12, and relevant experimental measures were determined.

### Cell culture

The primary neonatal mouse CFs were obtained from the hearts of 1- to 3-day-old newborn C57BL/6 mice. The isolated process was conducted following the steps outlined in previous literature.<sup>14</sup> According to the experimental protocol, CFs were exposed to high glucose (40 mM), SPD (10  $\mu$ M), and IL-17A (300 ng/ml).

### Serum and culture medium measurements

At each time point, the mouse's tail vein blood was used to measure blood glucose levels with a glucometer (GA-3, Sinocare, China). After 12 weeks of treatment, serum from each group of mice was separated and used to detect the following markers: insulin (Ziker, Shenzhen, China), triacylglycerol (TG) and total cholesterol (TC; Solarbio, Beijing, China), lactate dehydrogenase (LDH), creatine kinase isoenzyme (CK-MB), and cardiac troponin-I (cTnI; Solarbio, Beijing, China).

### Glucose tolerance tests

D-glucose (2-g/kg mass) was administered intraperitoneally to the mice after a 16-h fast. Blood glucose levels were measured at 15, 30, 60, 90, and 120 min using a glucometer (GA-3, Sinocare, China).

### Histology analysis

Mouse hearts were fixed in a 10% neutral formalin solution. The hearts were rinsed with deionized water and dehydrated with 70%, 80%, 95%, and 100% ethanol stepwise for 1.5 h at each level. After 3 h of wax immersion and 15 min of xylene transparency, the myocardial tissue was embedded in paraffin. The wax blocks were sliced into 4- $\mu$ m-thick sections with a slicer, and the tissue sections were baked for 3 h at 65 °C. Finally, the sections were dewaxed with xylene, followed by a stepwise dehydration process using 100%, 95%, 80%, and 70% ethanol. Hereafter, the staining experiments were performed as per the respective protocol.

### Echocardiographic analysis

Cardiac function and dimensions were evaluated using a 4D echocardiography machine (Mylab Delta-vet, Esaote, Italy). Echocardiography was performed on all mice under 2% isoflurane anesthesia, and relevant indicators of cardiac function were detected.

### Immunohistochemistry

The heart tissue sections of paraffin underwent a series of steps, including dewaxing, rehydration, and pretreatment with 10 mM citrate buffer at pH 6.0 for 3 min. Following this, the slices were incubated with 3% H<sub>2</sub>O<sub>2</sub> for 10 min, followed by exposure to the primary antibody of the target protein (diluted 1:250) overnight at 4 °C. Negative controls were performed using non-immune isotype IgG in place of primary antibodies. The sections were then treated with a secondary antibody (ABclonal Technology, Wuhan, China) for 1 h at 20 °C and stained with the DAB reagent. Eight separate images were captured in the region of interest without overlapping. The brown-stained areas in each image were quantified using ImageJ 1.46 software.

### Transmission electron microscopy

We used an ultrastructural analysis using the method described previously to visualize the collagen deposition.<sup>15</sup> In brief, the heart tissue was fixed, dehydrated, embedded, and examined using a transmission electron microscope to obtain observations (HT-7700, Hitachi, Japan).

### Bioinformatic analysis

Transcriptomic data analysis of DCM mouse heart tissue (GEO accession number: GSE161931) was performed using relevant bioinformatic analysis methods.<sup>16</sup> Cluster 3.0 software created a volcano plot and conducted a hierarchical clustering analysis. KEGG pathway was added, the DAVID Functional Annotation Chart tool (Version 6.8) performed KEGG enrichment analysis and GO enrichment.<sup>17,18</sup>

### Cell proliferation analysis

CFs were seeded in 12-well plates ( $1 \times 10^6$ ) and treated with or without high glucose (40 mM) and SPD (10  $\mu$ M). Subsequently, the CFs were incubated at 37 °C in EdU (Beyotime, Shanghai) medium (10  $\mu$ M). After a 24-h incubation, the cells were fixed and stained using the previous experimental method,<sup>19</sup> followed by 10-min staining with Hoechst 33342 at room temperature. Images were captured using a fluorescent microscope (IX53, OLYMPUS) and processed using ImageJ 1.46 software.

### Cell migration analysis

CFs were subjected to different treatments, and wounding healing assays were conducted by previously published procedures.<sup>20</sup> Images were captured at 0 and 24 h using phase-contrast microscopy.

Serum-free cell suspensions from each group were added to the chambers of a 24-well transwell plate (Biosharp, Hefei). Then, 500  $\mu$ l of DMEM containing 5% serum was added to the corresponding wells of the 24-well plate. After 24 h of culturing, the transwell chamber was removed, and the CFs were fixed with 5% polyformaldehyde for 30 min, followed by staining with 0.25% Coomassie brilliant blue for 5 min. The nonmigrated cells in the transwell chamber were gently wiped off using a cotton swab, and the chamber was washed three times with PBS. Migrated CFs were observed and captured in five visual fields using a microscope.

### Immunoprecipitation

CFs were inoculated in 35-mm culture dishes and underwent different treatments after 48 h. The CFs were lysed four times in RIPA lysis solution buffer (containing 1% PMSF) at 4 °C and shaken for 10 s every 10 min. The total protein was collected by centrifugation (4 °C, 13,500 r/min, 25 min), and 2  $\mu$ g of ubiquitination-specific antibodies (Santa Cruz Biotechnology, Inc.) were used for immunoprecipitation and then incubated with total protein lysate overnight at 4 °C. The target protein was extracted using the IP Protein A/G Magnetic Bead method, and its ubiquitination level was determined by Western blot analysis.

### siRNA transfection

The CFs were transfected with IL-17A-siRNA (Cat No. sc-39650, Santa Cruz Biotechnology) using PolyJet™ (Signagen). According to the published protocol, the relevant protein expression was suppressed for 6 h by incubating the transfection reagent in a serum-free medium. Subsequently, the serum-free medium was

replaced with DMEM (10% FBS), and further experiments could proceed.

### Western blot analysis

The experimental steps of Western blot were conducted by our previous literature.<sup>21</sup> The primary antibodies listed below were incubated with the membranes at 4 °C and stayed overnight (at a 1:1,000 dilution):  $\alpha$ -SMA, transforming growth factor (TGF)- $\beta$ 1, collagen-I, collagen-III, MMP-2, MMP-9, NLRP3, Caspase-1, GSDMD-N, interleukin (IL)-1 $\beta$ , IL-17A, and IL-18 (ABclonal Technology, Wuhan, China); ODC, SSAT, p-Smad-2, t-Smad-2, p-Smad-3, t-Smad-3, and Smad-7 (Cell Signaling Technology, Danvers, Massachusetts); and ubiquitin,  $\beta$ -actin, and  $\beta$ -tubulin (Santa Cruz Biotechnology). The membranes were incubated for 1 h at room temperature with secondary antibodies (diluted at 1:10,000, Proteintech, Wuhan, China). The specific complexes treated with an ECL kit (MultiSciences, Hangzhou, China) were detected using a multiplex fluorescent imaging system.

### Real-time PCR analysis

The Qiagen RNeasy mini kit was used to extract total RNA from myocardial tissue and CFs to assess the mRNA levels of target genes. A microgram of total RNA was then used for cDNA synthesis, and a 2- $\mu$ l portion (equivalent to 0.4- $\mu$ g cDNA) was subjected to PCR amplification using two suitable primers (Table 1). The  $\Delta\Delta$ CT method was used to measure the relative mRNA levels, with U6 as a reference and internal standard for quantification.

### Statistical analyses

Each experiment was independently replicated at least three times, and all data were presented as mean  $\pm$  SEM. Statistical analysis was conducted using GraphPad Prism 9.0, with either a two-tailed Student's t-test or one-way analysis of variance, followed by a Bonferroni multiple comparison test. A significance level of  $p < 0.05$  was considered statistically significant.

## RESULTS

### Exogenous SPD ameliorated cardiac functions in db/db mice

Eight-week-old WT mice and db/db mice were selected to explore the effects of SPD. SPD was provided via intraperitoneal injections every other day for 12 weeks. At week 12, we found that the related indicators and characteristic features of type 2 diabetes were positive. At each time point, the T2D and T2D + SPD groups had higher blood glucose levels and glucose intolerance than the WT group. Additionally, both groups exhibited a significant increase in insulin levels and significantly higher TG and TC levels. Surprisingly, there was no discernible difference in the indices mentioned above between the T2D and T2D + SPD groups (Figures 1a-f).

We analyzed serum myocardial injury markers to confirm that persistent hyperglycemia can result in significant cardiac damage. The results indicated that the T2D group had significantly higher serum CK-MB, cTnI, and LDH levels than the WT group. In contrast, the serum content of these enzymes was reduced in the

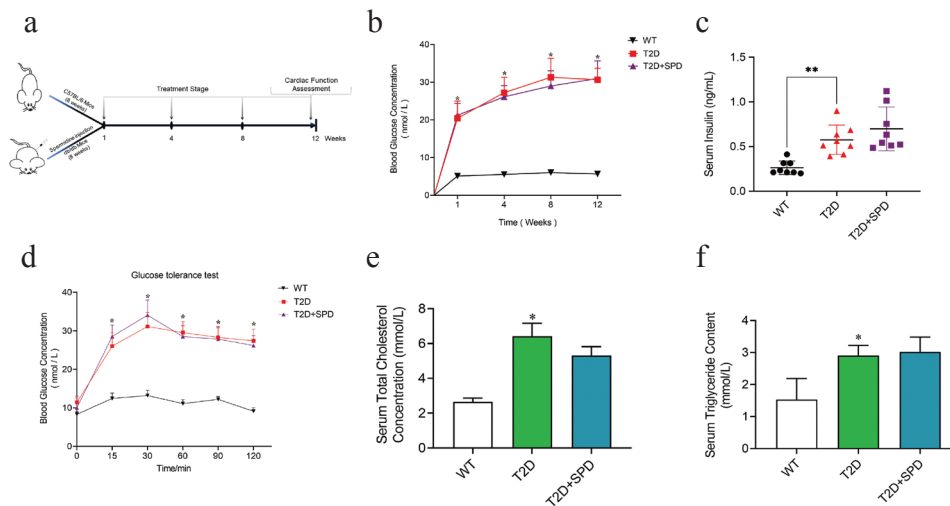


FIG. 1. Successful establishment of type 2 diabetic mouse model.

The db/db mouse was selected as the research participant to establish the T2D model, and the corresponding parameters were evaluated at the 12-week mark. (a) Scheme of the in vivo experiment, (b) blood glucose concentration, (c) serum insulin concentration, (d) insulin resistance test, (e) total cholesterol, and (f) triacylglycerol. \* $p < 0.05$  vs. WT group ( $n = 8$ ) and \*\* $p < 0.01$ .

T2D + SPD group compared with the T2D group. The above results implicate that SPD may have a protective and therapeutic effect on diabetic myocardial injury (Figures 2a-c). The echocardiography results indicated that the T2D + SPD group had higher EF and FS and lower LVIDs and LVIDd than the T2D group (Figures 2d-h). db/db mice had a higher BW than WT mice in the 12<sup>th</sup> week, and the administration of SPD did not affect BW (Figure 2i). Nevertheless, we discovered that SPD decreased HW/TL in the T2D group (Figure 2j).

### Exogenous SPD reduces myocardial fibrosis of the diabetic heart

In the 12<sup>th</sup> week, the hearts of mice in each group were extracted and analyzed using hematoxylin and eosin (H&E) staining. The staining results revealed that cardiac myocytes of db/db mice were disordered and hypertrophic (Figure 3a). The results of the Masson, Sirius Red staining, and transmission electron microscopy (TEM) revealed a significant accumulation of collagens in the heart of type 2 diabetic mice (Figure 3b), which was attenuated by SPD. Furthermore, IHC staining of cardiac tissue demonstrated a marked upregulation of collagen-I/III in the heart tissue of db/db mice, whereas SPD significantly suppressed the expression of both proteins (Figures 3c-f).

We used qRT-PCR to analyze the gene expression of collagen-I/III, Fibronectin, and Vimentin to investigate whether exogenous SPD affects collagen synthesis. Our results revealed a significant upregulation of these genes in the T2D group, whereas SPD significantly downregulated their expression levels (Figures 3g-j).

### Comparative transcriptomic analysis of cardiac tissues

There were 1,126 differentially expressed (DE) genes between C57BL/6 mice and db/db mice ( $p$  value  $< 0.05$ ), with 574

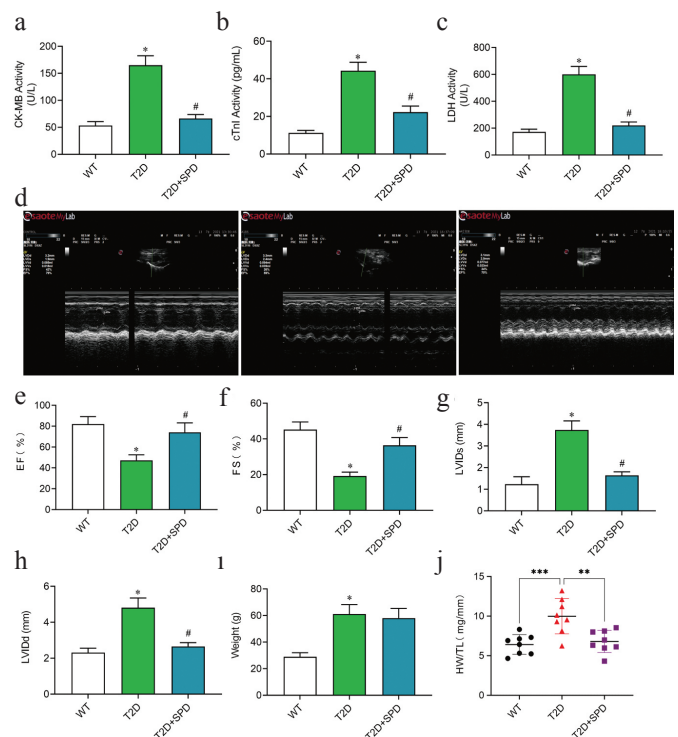


FIG. 2. SPD alleviates diabetic myocardial damage in the db/db mice. (a) Serum CK-MB concentration, (b) serum cTnI concentration, (c) serum lactate dehydrogenase concentration, (d) echocardiography, (e) left ventricular ejection fraction, (f) left fractional shortening, (g) left ventricular internal dimension diastole, (h) left ventricular internal dimension systole, (i) body weight, and (j) the ratio of heart weight to tibia length. \* $p < 0.05$  s. WT group, # $p < 0.05$  vs. T2D group ( $n = 8$ ), \*\* $p < 0.01$ , and \*\*\* $p < 0.001$ .

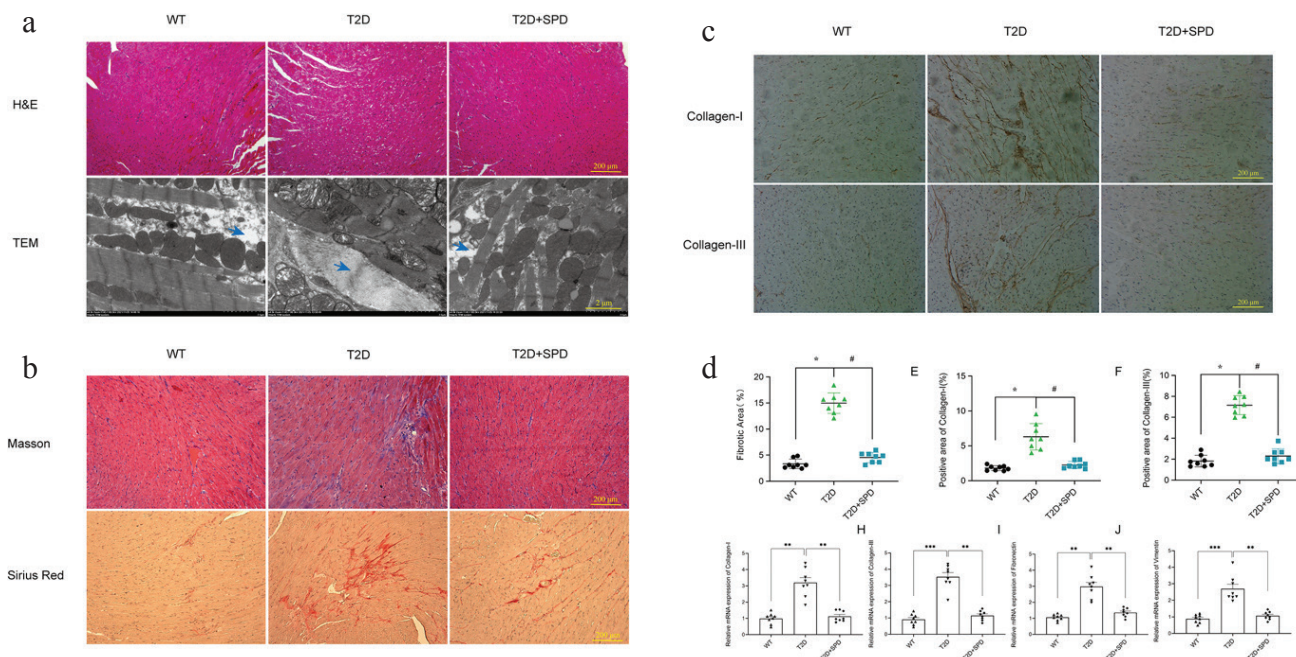


FIG. 3. SPD ameliorates diabetic cardiomyopathy by reducing collagen deposition in the db/db mice.

Twelve weeks after SPD injection in the db/db mice: (a) representative images of H&E staining and transmission electron microscopy (blue arrows indicate collagen deposition), (b) representative Masson's trichrome and Sirius Red staining of cross-sections of the heart tissues, (c) representative immunohistochemistry (IHC) detection of collagen-I and collagen-III, (d) myocardial fibrosis level, (e) expression of collagen-I was evaluated by IHC analysis, (f) expression of collagen-III was evaluated by IHC analysis, (g) mRNA expression of collagen-I, (h) mRNA expression of collagen-III, (i) mRNA expression of Fibronectin, and (j) mRNA expression of Vimentin. \* $p < 0.05$  vs. WT group, # $p < 0.05$  vs. T2D group ( $n = 8$ ), \*\* $p < 0.01$ , and \*\*\* $p < 0.001$ .

upregulated genes and 552 downregulated genes (Figure 4a). GO terms enrichment analysis was performed, and DE genes were identified to be enriched in the cell secretion and junction, extracellular matrix, lipid metabolism process, and inflammatory response process, all related to cellular components and biological processes (Figures 4b, c). Hereafter, DE genes were mapped to KEGG pathways, and the functional KEGG enrichment cluster image shows the top 10 enriched pathways (Figure 4d). The IL-17 signaling pathway caught our attention and became the primary subject of our study.

#### SPD restrains inflammation and pyroptosis in the diabetic mice

The metabolism of polyamines is regulated by ODC and SSAT. Compared with the C57BL/6 mice group, we observed that the former was downregulated and the latter was upregulated in the db/db mice group (Figure 5a). IHC and qRT-PCR results revealed that NLRP3, Caspase-1, GSDMD-N, and IL-1 $\beta$  were significantly upregulated in the T2D group. SPD could sensibly decrease the expression of these proteins and genes (Figures 5b, c).

#### SPD inhibits CFs from secreting collagens, migration, and proliferation

We evaluated the expression of  $\alpha$ -SMA, collagen-I/III, and MMP-2/9 (the main markers of myocardial fibrosis) to verify the effects of exogenous SPD on the biological properties of CFs. Our

findings showed that these proteins were significantly upregulated in the HG group and treatment with SPD could significantly downregulate their expressions (Figure 6a). Cell migration results confirmed that HG and SPD had to promote and inhibit effects on the migration of CFs, respectively (Figures 6b, c). We also evaluated the proliferation of CFs using the EdU assay and found that the proliferation ability of cells was increased when treated with HG, but SPD treatment could significantly reduce it (Figure 6d).

#### SPD inhibits collagen synthesis via suppressing pyroptosis and Smad-7 ubiquitination

Based on the previous transcriptomic analysis, we focused on the genes related to pyroptosis to further elucidate the mechanism of CFs overexpressing collagens in DCM. We found a significant upregulation of NLRP3, Caspase-1, GSDMD-N, IL-1 $\beta$ , IL-17, and IL-18 expression in the HG group, whereas treatment with SPD caused a significant decrease in this protein expression (Figure 7a). Moreover, HG increased TGF- $\beta$ 1 and p-Smad-2/3 expression and decreased Smad-7 expression, but SPD exhibited significant inhibitory effects on their expression (Figure 7b). These findings suggest that SPD can inhibit pyroptosis and fibrotic pathway activation.

The whole-cell ubiquitination levels were analyzed using Western blot. It was revealed that HG increased the ubiquitination levels, whereas SPD had the reverse effect. The co-immunoprecipitation

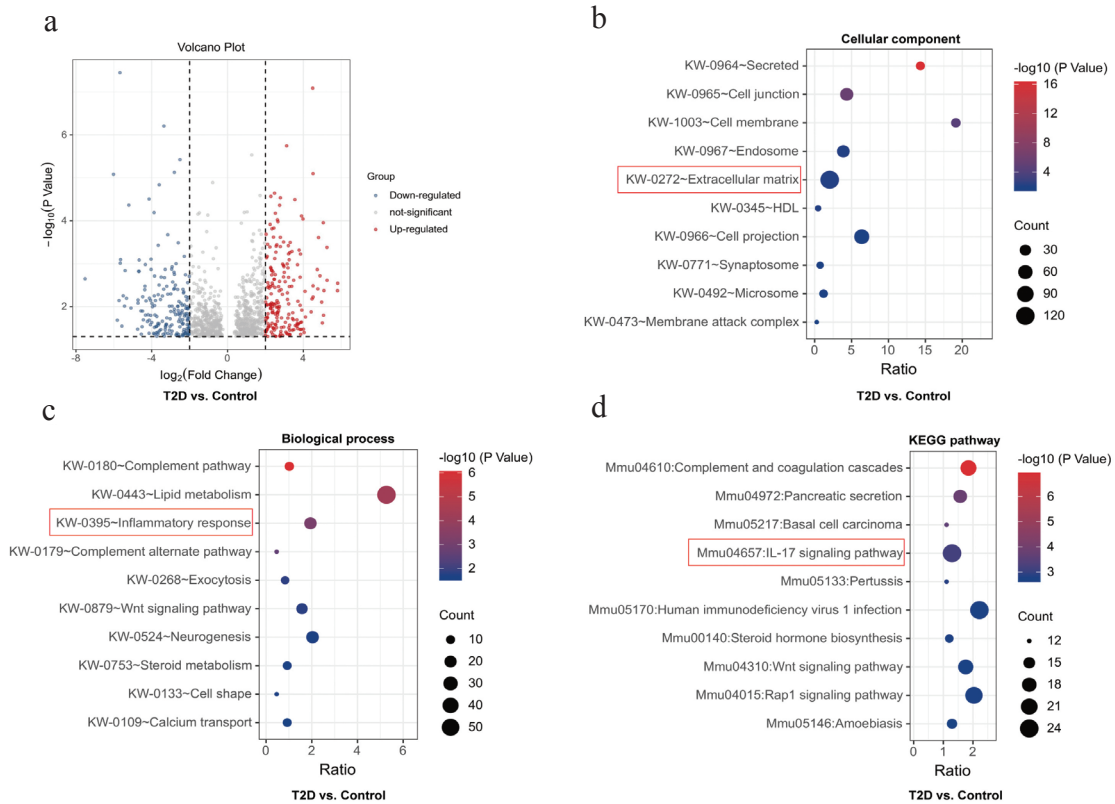


FIG. 4. Transcriptomic analysis of the cardiac tissues from C57BL/6 mice and db/db mice. (a) Volcano plot showing the quantitative gene expression in the cardiac tissues from C57BL/6 mice and db/db mice and differential protein expression with a fold change of >1.5 are marked in color, (b) cellular component analysis, (c) biological process analysis, and (d) KEGG enrichment analysis for all the aberrantly expressed genes. \* $p < 0.05$  vs. WT group and # $p < 0.05$  vs. T2D group ( $n \geq 3$ ).

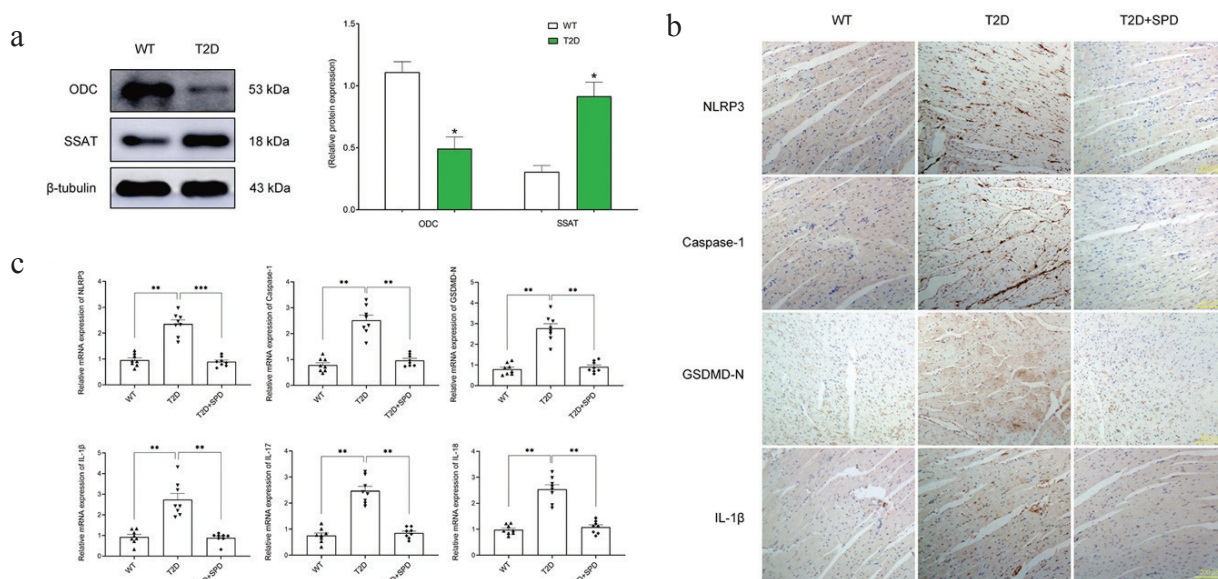


FIG. 5. SPD inhibits inflammation and pyroptosis in T2D mice. The transcriptomic analysis results show that diabetic cardiomyopathy is involved in the inflammatory pathway. (a) Representative Western blot of ODC and SSAT in comparison with  $\beta$ -tubulin expression in the myocardial tissues, (b) representative immunohistochemistry of NLRP3, Caspase-1, GSDMD-N, and IL-1 $\beta$ , and (c) mRNA expression of NLRP3, Caspase-1, GSDMD-N, IL-1 $\beta$ , IL-17, and IL-18 analyzed by qRT-PCR. \* $p < 0.05$  s. WT group, # $p < 0.05$  vs. T2D group ( $n \geq 3$ ), \*\* $p < 0.01$ , and \*\*\* $p < 0.001$ .

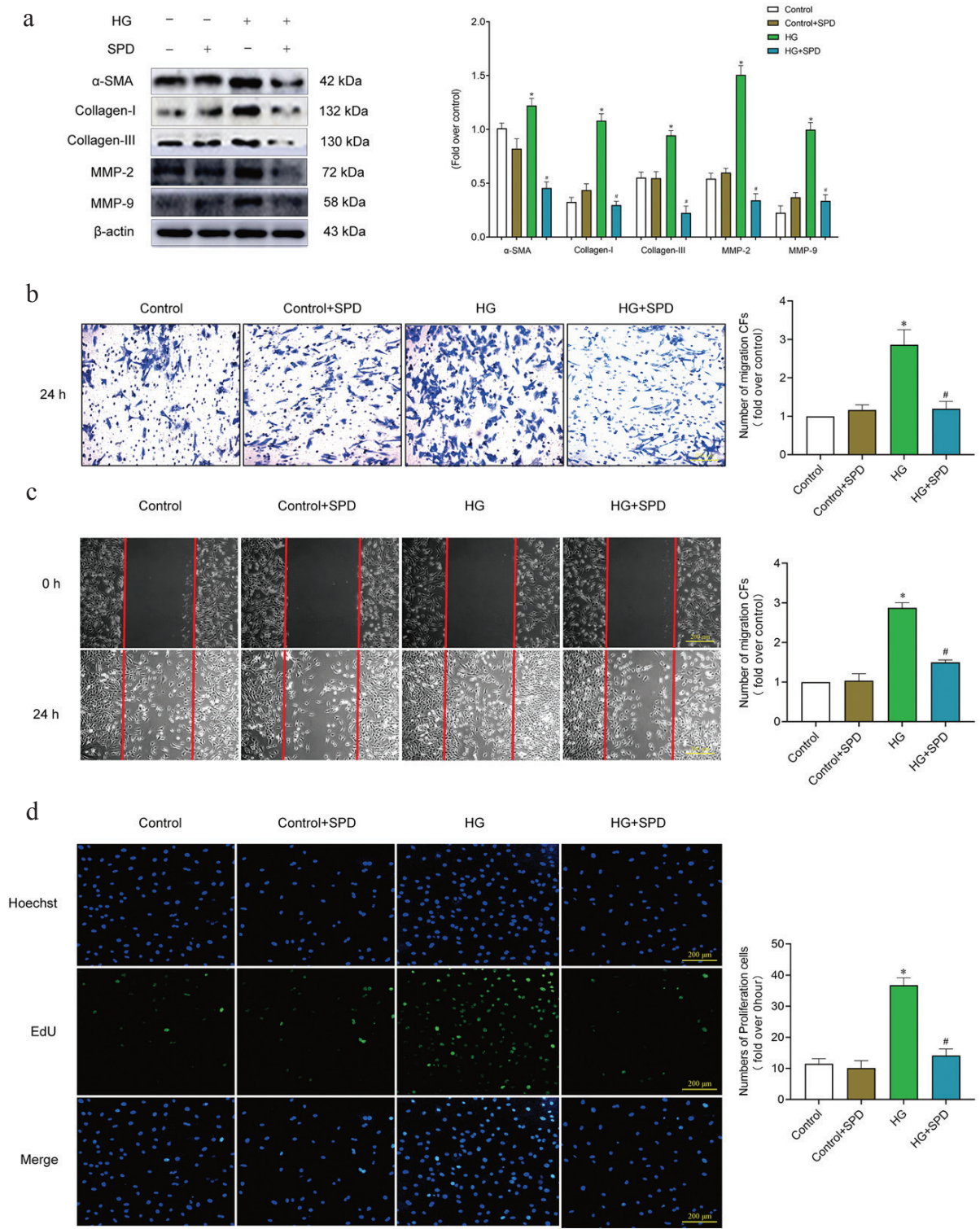


FIG. 6. Effects of SPD on proliferation and migration of the cardiac fibroblasts (CFs). CFs were cultured for 24 h in a control group (5.5 mM), control + SPD group (10  $\mu$ M), HG group (40 mM), and HG + SPD (10  $\mu$ M) group. (a) Western blot evaluated the expression of  $\alpha$ -SMA, collagen-I, collagen-III, MMP-2, and MMP-9. (b) Transwell assay was used to detect the CF migration. (c) CFs migration was assessed by scratch wound repair. (d) EdU detected the proliferation of CFs. \* $p < 0.05$  vs. control group and # $p < 0.05$  vs. IL-17A group ( $n \geq 3$ ), \*\* $p < 0.01$ , and \*\*\* $p < 0.001$ .

results showed that HG could increase Smad-7 ubiquitination, whereas SPD markedly inhibited it (Figures 7c, d). Subsequently, we treated the CFs with IL-17A and found that IL-17A could increase both the whole-cell and Smad-7 ubiquitination levels (Figures 7e, f). Furthermore, cell migration assays confirmed that the migration ability of CFs was increased in the IL-17A group, while it was significantly decreased in the IL-17A + SPD group (Figure 8a). The EdU detections demonstrated that the cell proliferation numbers were increased in the IL-17A group but were significantly decreased in the IL-17A + SPD group (Figure 8b). We further validated the results by measuring the expression of collagen-I/III, Fibronectin, and Vimentin. We found that these genes were upregulated in the IL-17A group. Treatment with SPD and si-IL-17A could significantly downregulate the genes mentioned above (Figures 8c, d).

**DISCUSSION**

For this study, we chose knocked-out diabetes gene mice as our research participants. These mice are a commonly used mouse model of type 2 diabetes and are widely used in research on endocrine dysfunctions, neurological disorders, and cardiac ailments caused by dysglycemia and dyslipidemia. At each time point, the db/db mice had persistent hyperglycemia, and no decrease was observed after the SPD injection. After 12 weeks, the T2D group showed a large increase in insulin activity and a significant rise in TC and TG serum content. These findings were consistent with the results of the insulin resistance test. Interestingly, SPD had no impact on the indicators above.

After a myocardial injury, blood injury markers increase, and echocardiography reveals abnormalities. Myocardial injury markers were significantly elevated in the db/db mouse heart. Additionally, echocardiography revealed a decrease in EF and FS and an increase in LVIDs and LVIDd, indicating systolic dysfunction of the heart. Notably, treatment with SPD improved this dysfunction. The type 2 diabetic mice also exhibited a significant increase in body weight. Subsequently, we were surprised that SPD only decreased the HW/TL ratio, which may be attributed to heart remodeling and increased extracellular matrix. The following series of experiments validate this supposition. Collagen staining revealed substantial collagen deposition in the interstitial areas of diabetic hearts. TEM results also showed apparent collagen deposition in the internal space of the cardiomyocyte structure, whereas H&E staining revealed cardiomyocyte degeneration and necrosis in the db/db mouse heart. However, SPD was effective in inhibiting these changes. The above experimental phenomena have also been confirmed in the results of IHC and qRT-PCR results. These findings show that SPD has a positive therapeutic effect on myocardial injury and fibrosis repair.

Enrichment analysis of GO terms and KEGG was performed, showing that myocardial remodeling was closely related to the synthesis of extracellular matrix, inflammatory response, and IL-17 signaling pathway, which led us to the prospects of our present study. According to recent literature, activating the IL-17 signaling pathway can promote pyroptosis, a programmed cell death linked with an inflammatory response characterized by cellular swelling and fragmentation.<sup>22,23</sup> The pathological process is primarily

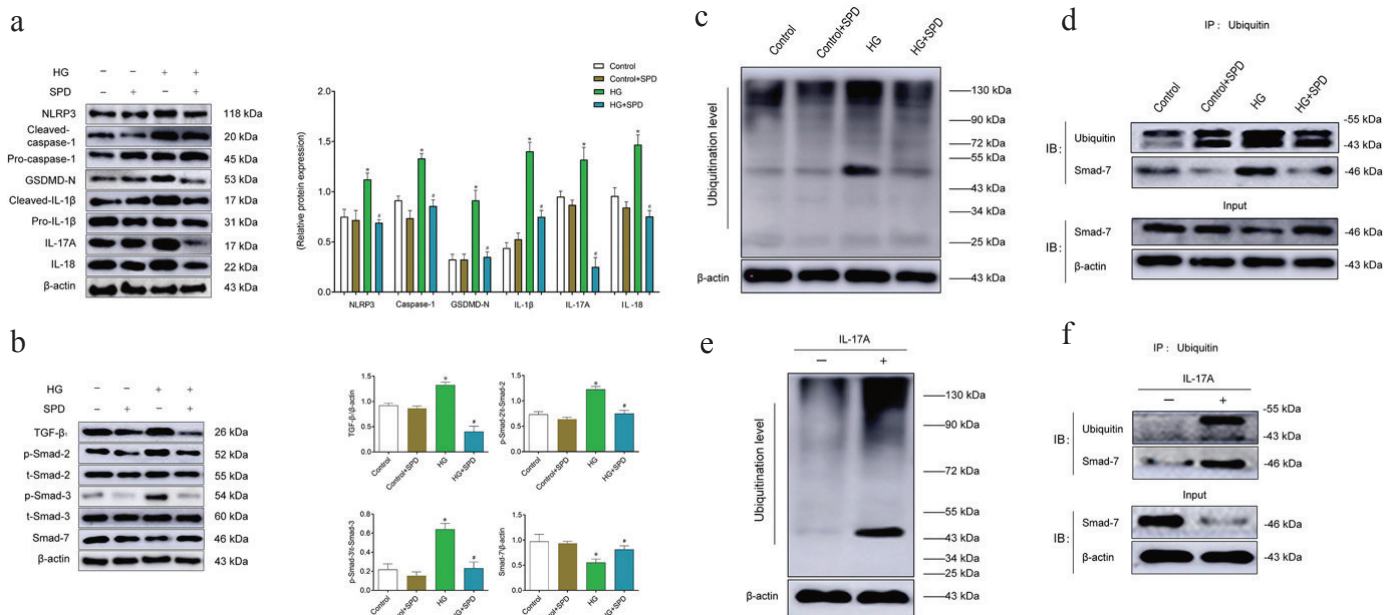


FIG. 7. SPD suppresses pyroptosis and Smad-7 ubiquitination levels. (a) Representative Western blot of NLRP3, Caspase-1, GSDMD-N, IL-1β, IL-17A, and IL-18 in comparison with β-actin expression, (b) representative Western blot of TGF-β1 in comparison with β-actin expression, p-Smad-2 in comparison with t-Smad-2 expression, p-Smad-3 in comparison with t-Smad-3 expression in CFs, and Smad-7 in comparison with β-actin expression, (c) whole-cell ubiquitination level determined by Western blot, (d) Smad-7 ubiquitination level determined by Western blot, (e) whole-cell ubiquitination level in CFs treated with IL-17A, and (f) Smad-7 ubiquitination level in CFs treated with IL-17A. \*p < 0.05 vs. control group and #p < 0.05 vs. HG group (n ≥ 3).

achieved by the caspase-1-dependent canonical inflammation pathway and the caspase-4/5/11-dependent non-canonical inflammation pathway. Several studies have shown that IL-1 $\beta$ , IL-18, and Gasdermin D (GSDMD) are the key proinflammatory cytokines that lead to inflammasome activation, thus resulting in pyroptosis-mediated cell death.<sup>24,25</sup> Moreover, NLRP3 is a member of the NOD-like receptor family, which can form an inflammasome and activate caspase-1 to release the inflammatory factors that cause pyroptosis.<sup>26</sup> We found that key proteins and genes in the pyroptosis pathway were significantly upregulated in the hearts of diabetic mice. SPD intervention effectively inhibited the above changes, demonstrating SPD's anti-inflammatory, anti-pyroptotic, and cardioprotective effects.

Our previous study confirmed that SPD could suppress ROS, ERS, and ferroptosis to alleviate diabetic myocardial injury caused by cardiomyocyte loss or necrosis.<sup>27</sup> CFs are also important in heart injury. In diseased hearts,<sup>28,29</sup> CFs transform into myofibroblasts

through activation or EMT, which are shaped like dendrites or spindles and have an increased ability to secrete collagen. Therefore,  $\alpha$ -SMA activation can be used as a specific marker protein in the transformation process. A high concentration of glucose as an injury factor in a diabetic organism can stimulate the excessive proliferation and differentiation of CFs, resulting in  $\alpha$ -SMA overexpression, an extracellular matrix disorder, and a severe imbalance in the ratio of collagen-I/III, which is the leading cause of myocardial fibrosis in DCM.<sup>30</sup> We subsequently uncovered that treatment with SPD could inhibit the occurrence of myocardial fibrosis.

According to a previous study,<sup>31</sup> myocardial fibrosis is closely related to the activation of the TGF- $\beta$ 1/Smad signaling pathway. Recent research has shown that an inflammatory response can activate the classic fibrotic pathway and transform fibroblasts into myofibroblasts, leading to collagen deposition and increasing myocardial remodeling and fibrosis.<sup>32,33</sup> More importantly, IL-17A

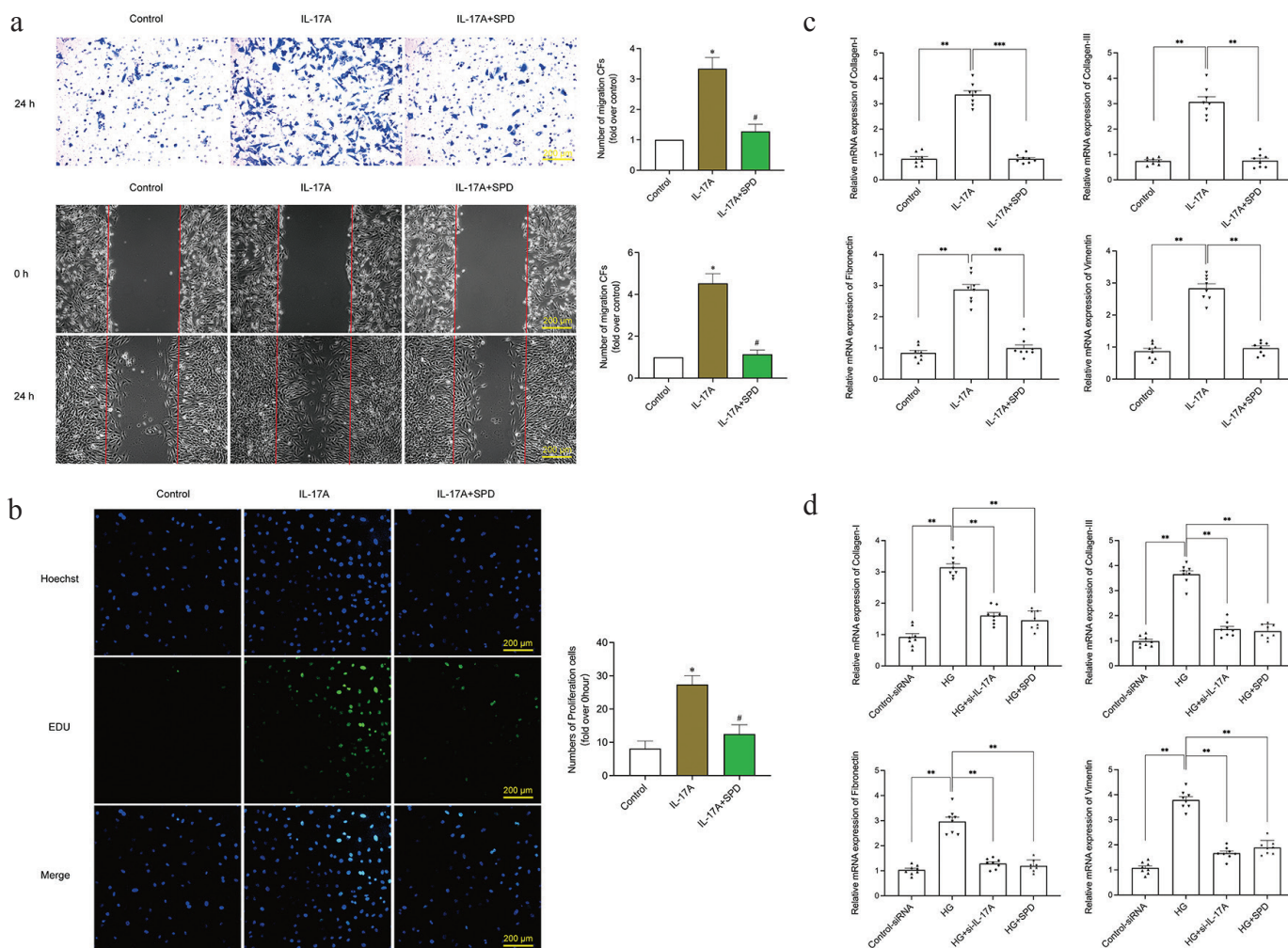


FIG. 8. IL-17A increases the proliferation and migration of the cardiac fibroblasts (CFs). CFs were treated with HG (40 mM), IL-17A (300 ng/mL), and SPD (10  $\mu$ M) for 24 h. (a) CF migration was detected using transwell assay and scratch wound repair, (b) proliferation of cardiac fibroblasts was detected by EdU, (c) mRNA expression of collagen-I, collagen-III, Fibronectin, and Vimentin, and (d) mRNA expression of collagen-I, collagen-III, Fibronectin, and Vimentin detected by qRT-PCR. \* $p$  < 0.05 vs. control group, # $p$  < 0.05 vs. HG group ( $n \geq 3$ ), and \*\* $p$  < 0.01.

induced NLRP3 formation and activation, releasing IL-1 $\beta$  and IL-18 from inflammatory cells and leading to cell pyroptosis.<sup>34</sup> In vitro, we found that HG could increase the expression of key inflammatory factors, and SPD had a strong anti-inflammatory effect. Subsequently, we demonstrated that SPD could prevent the Smad-2/3 complex from combining. The results of co-immunoprecipitation also confirmed that SPD could decrease the ubiquitination level of Smad-7 (an inhibitory Smad), which inhibits the activation of the TGF- $\beta$ 1/Smad signaling pathway and thus suppress collagen synthesis; however, stimulation of IL-17A showed the opposite effects to the treatment of SPD.

Based on the experimental findings and existing literature discussed earlier, a hypothesis can be formulated that continuous hyperglycemic stimulation can cause damage to the myocardium and provoke an inflammatory response, leading to pyroptotic cell death in db/db mice. Subsequently, inflammatory factors induce CF proliferation and increase Smad-7 ubiquitination levels to activate TGF- $\beta$ 1/Smad pathway following the transitional collagen deposition. Encouragingly, the abovementioned molecular regulation processes can be reversed by SPD. In the future, these findings should provide new targets and an empirical foundation for preventing and treating diabetic myocardial fibrosis.

**Ethics Committee Approval:** Mudanjiang Medical University (MMU) Medical Science Ethics Committee (20220516-17).

**Data Sharing Statement:** The data that support the findings of this study are available from the corresponding author upon reasonable request.

**Authorship Contributions:** Concept- H.Y.; Data Collection and Processing- C.W., J.X., J.Q., S.Z.; Analysis or Interpretation- C.W., J.X., J.Q., S.Z., H.Y.; Literature Search- Y.L.; Writing- H.Y.

**Conflict of Interest:** No conflict of interest was declared by the authors.

**Funding:** This research is supported by Heilongjiang Natural Science Foundation Project (no: LH2022H097); The Basic Scientific Research Business Research Project of Heilongjiang (no: 2021-KYYWF-0466); Doctoral Research Start-up Fund Project of Mudanjiang Medical University (no: 2021-MYBSKY-040); The National Natural Science Foundation of China (no: 82170268).

## Supplementary TABLE 1.

<http://balkanmedicaljournal.org/uploads/pdf/-SUPPLEMENT-TABLE-1.pdf>

## REFERENCES

- Rubler S, Dlugash J, Yuceoglu YZ, Kumral T, Branwood AW, Grishman A. New type of cardiomyopathy associated with diabetic glomerulosclerosis. *Am J Cardiol.* 1972;30:595-602. [CrossRef]
- Cai Z, Yuan S, Luan X, et al. Pyroptosis-Related Inflammasome Pathway: a new therapeutic target for diabetic cardiomyopathy. *Front Pharmacol.* 2022;13:842313. [CrossRef]
- Yuan H, Fan Y, Wang Y, et al. Calcium-sensing receptor promotes high glucose-induced myocardial fibrosis via upregulation of the TGF- $\beta$ 1/Smads pathway in cardiac fibroblasts. *Mol Med Rep.* 2019;20:1093-1102. [CrossRef]
- Wang J, Li S, Wang J, et al. Spermidine alleviates cardiac aging by improving mitochondrial biogenesis and function. *Aging (Albany NY).* 2020;12:650-671. [CrossRef]
- Chai N, Zhang H, Li L, Spermidine prevents heart injury in neonatal rats exposed to intrauterine hypoxia by inhibiting oxidative stress and mitochondrial fragmentation. *Oxid Med Cell Longev.* 2019;2019:5406468. [CrossRef]
- Stewart TM, Dunston TT, Woster PM, Casero RA. Polyamine catabolism and oxidative damage. *J Biol Chem.* 2018;293:18736-18745. [CrossRef]
- Zou T, Rao JN, Guo X, et al. NF-kappaB-mediated IAP expression induces resistance of intestinal epithelial cells to apoptosis after polyamine depletion. *Am J Physiol Cell Physiol.* 2004;286:1009-1018. [CrossRef]
- Madeo F, Carmona-Gutierrez D, Kepp O, Kroemer G. Spermidine delays aging in humans. *Aging (Albany NY).* 2018;10:2209-2211. [CrossRef]
- Jing YH, Yan JL, Wang QJ, et al. Spermidine ameliorates the neuronal aging by improving the mitochondrial function in vitro. *Exp Gerontol.* 2018;108:77-86. [CrossRef]
- Wang JY, Ma D, Luo M, et al. Effect of spermidine on ameliorating spermatogenic disorders in diabetic mice via regulating glycolysis pathway. *Reprod Biol Endocrinol.* 2022;20:45. [CrossRef]
- Hu J, Lu X, Zhang X, Shao X, Wang Y, Chen J, et al. Exogenous spermine attenuates myocardial fibrosis in diabetic cardiomyopathy by inhibiting endoplasmic reticulum stress and the canonical Wnt signaling pathway. *Cell Biology International.* 2020;44(8):1660-70. [CrossRef]
- Wang Y, Wang Y, Li F, et al. Spermine protects cardiomyocytes from high glucose-induced energy disturbance by targeting the CaSR-gp78-ubiquitin proteasome system. *Cardiovasc Drugs Ther.* 2021;35:73-85. [CrossRef]
- Wang Y, Chen J, Li S, et al. Exogenous spermine attenuates rat diabetic cardiomyopathy via suppressing ROS-p53 mediated downregulation of calcium-sensitive receptor. *Redox Biol.* 2020;32:101514. [CrossRef]
- Sun J, Xu J, Liu Y, et al. Exogenous spermidine alleviates diabetic cardiomyopathy via suppressing ROS, ERS and Pannexin-1-mediated ferroptosis. *Biomol Biomed.* 2023. [CrossRef]
- Yuan H, Xu J, Zhu Y, et al. Activation of calcium-sensing receptor-mediated autophagy in high glucose-induced cardiac fibrosis in vitro. *Mol Med Rep.* 2020;22:2021-2031. [CrossRef]
- Huang X, Zhang KJ, Jiang JJ, Jiang SY, Lin JB, Lou YJ. Identification of Crucial Genes and Key Functions in Type 2 Diabetic Hearts by Bioinformatic Analysis. *Front Endocrinol (Lausanne).* 2022;13:801260. [CrossRef]
- Sun Y, Zhang L, Lu B, et al. Hydrogen sulphide reduced the accumulation of lipid droplets in cardiac tissues of db/db mice via Hrd1 S-sulfhydration. *J Cell Mol Med.* 2021;25:9154-9167. [CrossRef]
- Zhang Y, Zhang S, Li B, et al. Gut microbiota dysbiosis promotes age-related atrial fibrillation by lipopolysaccharide and glucose-induced activation of NLRP3-inflammasome. *Cardiovasc Res.* 2022;118:785-797. [CrossRef]
- Yuan H, Xu J, Zhu Y, et al. Activation of calcium-sensing receptor-mediated autophagy in high glucose-induced cardiac fibrosis in vitro. *Mol Med Rep.* 2020;22:2021-2031. [CrossRef]
- Liang CC, Park AY, Guan JL. In vitro scratch assay: a convenient and inexpensive method for analysis of cell migration in vitro. *Nat Protoc.* 2006;2:329-333. [CrossRef]
- Sun J, Xu J, Liu Y, et al. Proteomic and metabolomic analyses reveal the novel targets of spermine for alleviating diabetic cardiomyopathy in type II diabetic mice. *Front Cardiovasc Med.* 2022;9:1022861. [CrossRef]
- Place DE, Kanneganti TD. Cell death-mediated cytokine release and its therapeutic implications. *J Exp Med.* 2019;216:1474-1486. [CrossRef]
- Li LL, Dai B, Sun YH, Zhang TT. The activation of IL-17 signaling pathway promotes pyroptosis in pneumonia-induced sepsis. *Ann Transl Med.* 2020;8:674. [CrossRef]
- Kesavardhana S, Kanneganti TD. Mechanisms governing inflammasome activation, assembly and pyroptosis induction. *Int Immunol.* 2017;29:201-210. [CrossRef]
- Al Mamun A, Mimi AA, Zaeem M, et al. Role of pyroptosis in diabetic retinopathy and its therapeutic implications. *Eur J Pharmacol.* 2021;904:174166. [CrossRef]
- Mangan MS, Olhava EJ, Roush WR, Seidel HM, Glick GD, Latz E. Targeting the NLRP3 inflammasome in inflammatory diseases. *Nat Rev Drug Discov.* 2018;17:588-606. [CrossRef]
- Sun J, Xu J, Liu Y, et al. Exogenous spermidine alleviates diabetic cardiomyopathy via suppressing ROS, ERS and Pannexin-1-mediated ferroptosis. *Biomol Biomed.* 2023. [CrossRef]

28. Zhang Y, Lu Y, Ong'achwa MJ, et al. Resveratrol inhibits the TGF- $\beta$ 1-induced proliferation of cardiac fibroblasts and collagen secretion by downregulating miR-17 in rat. *Biomed Res Int.* 2018;2018:8730593. [\[CrossRef\]](#)
29. Wang L, Jiang P, He Y, et al. A novel mechanism of Smads/miR-675/TGF $\beta$ R1 axis modulating the proliferation and remodeling of mouse cardiac fibroblasts. *J Cell Physiol.* 2019;234:20275-20285. [\[CrossRef\]](#)
30. Zhang D, Cui Y, Li B, Luo X, Li B, Tang Y. miR-155 regulates high glucose-induced cardiac fibrosis via the TGF- $\beta$  signaling pathway. *Mol BioSyst.* 2017;13:215-224. [\[CrossRef\]](#)
31. Yuan H, Fan Y, Wang Y, Gao T, Shao Y, Zhao B, et al. Calcium-sensing receptor promotes high glucose-induced myocardial fibrosis via upregulation of the TGF- $\beta$ 1/Smads pathway in cardiac fibroblasts. *Mol Med Rep.* 2019;20:1093-1102. [\[CrossRef\]](#)
32. Luo DD, Fielding C, Phillips A, Fraser D. Interleukin-1 beta regulates proximal tubular cell transforming growth factor beta-1 signalling. *Nephrol Dial Transplant.* 2009;24:2655-2665. [\[CrossRef\]](#)
33. Chaudhuri V, Zhou L, Karasek M. Inflammatory cytokines induce the transformation of human dermal microvascular endothelial cells into myofibroblasts: a potential role in skin fibrogenesis. *J Cutan Pathol.* 2007;34:146-153. [\[CrossRef\]](#)
34. Li Y, Chang LH, Huang WQ, et al. IL-17A mediates pyroptosis via the ERK pathway and contributes to steroid resistance in CRSwNP. *J Allergy Clin Immunol.* 2022;150:337-351. [\[CrossRef\]](#)